

## Dynamic neutron sources from the $^{207}\text{Pb}(\gamma,n)$ and $^{205}\text{Tl}(\gamma,n)$ reactions

Sylvian Kahane <sup>a</sup>, Yair Ben-Dov (Birenbaum) <sup>b</sup>, Raymond Moreh <sup>c</sup>

<sup>a</sup> *P.O. Box 1630, 84965, Omer, Israel*

<sup>b</sup> *Nuclear Research Center, Negev, 84190, Beer-Sheva, Israel*

<sup>c</sup> *Department of Physics, Ben-Gurion University, 84120, Beer-Sheva, Israel*

### ABSTRACT

Mono-energetic  $\gamma$ -beams ( $\Delta \sim 10$  eV) based on thermal neutron capture, in a nuclear reactor, using the  $\text{V}(n,\gamma)$  and  $\text{Fe}(n,\gamma)$  reactions were utilized for generating fast neutron sources from lead and thallium respectively, via the  $^{207}\text{Pb}(\gamma,n)$  and  $^{205}\text{Tl}(\gamma,n)$  reactions. It so happened that one of the incident  $\gamma$ -lines of the V source,  $E_\gamma = 7163$  keV, photoexcites by chance a resonance level in  $^{207}\text{Pb}$ , which emits neutrons at an energy of 423 keV. In a similar manner the incident  $\gamma$ -line at  $E_\gamma = 7646$  keV of the  $\text{Fe}(n,\gamma)$  source photoexcites by chance a resonance level in the  $^{205}\text{Tl}$  isotope, which emits neutrons at an energy of 99 keV. The cross sections for the neutron emission process were measured and found to be  $\sigma(\gamma,n) = 35 \pm 6$  mb and  $107 \pm 17$  mb respectively with intensities of the order of  $10^4$  n/sec.

**Keywords:**  $\gamma$ -ray beams;  $\text{V}(n,\gamma)$  reaction;  $\text{Fe}(n,\gamma)$  reaction;  $^{207}\text{Pb}(\gamma,n)$  reaction;  $^{205}\text{Tl}(\gamma,n)$  reaction; Nuclear Reactor

-----

Email addresses: [sylviankahane@gmail.com](mailto:sylviankahane@gmail.com) (S. Kahane), [bendovori@gmail.com](mailto:bendovori@gmail.com) (Y. Ben-Dov), [moreh@bgu.ac.il](mailto:moreh@bgu.ac.il) (R. Moreh)

## 1. Introduction

Neutron sources may be induced by the  ${}^9\text{Be}(\alpha, n)$  reaction using alpha emitters such as  ${}^{210}\text{Po}$ ,  ${}^{239}\text{Pu}$ ,  ${}^{226}\text{Ra}$ ,  ${}^{241}\text{Am}$  and  ${}^{242}\text{Cm}$ ; such sources are prepared by mixing the  ${}^9\text{Be}$  with any of the above alpha emitters<sup>1-4</sup>. Another class of n-sources are based on the  ${}^9\text{Be}(\gamma, n)$  reaction<sup>3,4</sup> where the gamma-rays are obtained from radioactive isotopes such as  ${}^{124}\text{Sb}$ , which emit  $\gamma$ -rays of energies higher than 1.665 MeV being the threshold for n-emission in  ${}^9\text{Be}$ . Other sources based on spontaneous fission of heavy nuclei, e.g.  ${}^{252}\text{Cf}$ , are also used<sup>4</sup>. In addition, there are numerous accelerator-based neutron sources: using e.g. protons obtained from a van de Graaff accelerators ( $E_p = 3$  MeV) and employing the  ${}^7\text{Li}(p, n){}^7\text{Be}$  reaction which generates neutrons in the 0 to 1.3 MeV energy range<sup>5</sup>. Other particle accelerators vary in size and diversity including large installations such as the Spallation pulsed Neutron Source at Rutherford Laboratory which employ 2 GeV protons for generating huge fluxes of continuous energy neutrons<sup>6</sup>. Another pulsed neutron source using 20 GeV protons is the neutron time-of-flight facility, n\_TOF, which operates at CERN producing high-intensity neutron beams having wide energy range of energies from a few meV to several GeV<sup>7</sup>.

Electrons at  $E_e \sim 50$  MeV are also used for producing photoneutrons via bremsstrahlung as in the Gaertner Linear Accelerator Laboratory at Rensselaer Polytechnic Institute. The energy determination of neutrons is made using time of flight. A filter of pure iron is employed to convert a white neutron spectrum to a neutron beam with several discrete energies between 24.3 keV to 938 keV<sup>8</sup>. In addition, a pure  ${}^{238}\text{U}$  filter is also used generating a multi-line neutron beam in the range 34 eV to 6.2 keV<sup>9</sup>.

In this work, we deal with neutron sources based on the  $(\gamma, n)$  reactions on various elements using high energy photons of 7 to 10 MeV produced by thermal n-capture in a nuclear reactor<sup>10-12</sup>. The production of such a neutron source requires three stringent conditions: (1) one of the incident  $\gamma$ -lines produced by the  $(n, \gamma)$  source should resonantly photoexcite, *by chance, an isolated* nuclear level in the target; (2) The photoexcited level should be an *unbound* level higher than the threshold energy for neutron emission; (3) the cross section for n-emission should be high enough for producing a neutron source of relatively high intensity. Here we deal with two neutron sources: The first is based on the  $V(n, \gamma)$  reaction where the 7.163 MeV gamma ray is generated by thermal neutron capture in  ${}^{51}\text{V}$  with subsequent deexcitation to the 147.8 keV level of  ${}^{52}\text{V}$ . This  $\gamma$  line happens to photoexcite resonantly an unbound level in  ${}^{207}\text{Pb}$  inducing a  ${}^{207}\text{Pb}(\gamma, n){}^{206}\text{Pb}$  reaction which leaves the residual  ${}^{206}\text{Pb}$  nucleus (Fig. 3) at its ground state with the emission of the 423

keV neutron group (there is a small spread in energy due to the kinematics). The second source is similar, thermal neutron capture in  $^{56}\text{Fe}$  produces a 7.646 MeV  $\gamma$  with the resulting  $^{57}\text{Fe}$  at the ground state.  $^{205}\text{Tl}$  is resonantly photoexcited by this gamma, emits neutrons at  $E_n = 99$  keV while the residual  $^{204}\text{Tl}$  is left at the ground state (Fig. 6). These sources are “dynamic n-sources” in the sense that can be produced only when a nuclear reactor is operated, creating photons via the  $V(n,\gamma)$  or  $\text{Fe}(n,\gamma)$  reactions followed by neutrons via the  $(\gamma,n)$  reaction.

Such accidental photoexcitation processes are not very rare. This may be understood if one considers the large number of the discrete  $\gamma$  lines in each photon beam and also the density of nuclear levels occurring in each nucleus at excitations of 7 to 10 MeV. Both the incident  $\gamma$  line and the nuclear level are Doppler broadened having  $\Delta \sim 10$  eV where the broadening depends on the energy and the nuclear mass, as explained in Sec. 3.3 below.

In the past, few photoneutron studies using n-capture gamma rays<sup>13</sup> were carried out. Studies of neutron emitting resonance levels (by photoexcitation of isolated *resonance* levels) were reported in Ref. 14-17. In Ref. 14 a  $\gamma$  line at 7632 keV of the  $\text{Fe}(n,\gamma)$  reaction photoexcites one nuclear level in  $^{207}\text{Pb}$  producing a strong dynamic neutron source having  $E_n = 86$  keV<sup>14</sup>. In Ref. 15 the  $\gamma$  line at 7637 keV of the  $\text{Cu}(n,\gamma)$  reaction overlaps a nuclear level in  $^{209}\text{Bi}$  emitting strong intensity neutron groups at  $E_n = 114$  keV and 177 keV<sup>15</sup>. In Ref. 16, a  $\gamma$ -line at 8884 keV of the  $\text{Cr}(n,\gamma)$  reaction photoexcites a level in  $^{49}\text{Ti}$  emitting neutrons at  $E_n = 726$  keV<sup>16</sup>. Finally in Ref. 17  $^{208}\text{Pb}$  was photoexcited by the 7632 keV  $\gamma$ -line of the  $\text{Fe}(n,\gamma)$  reaction emitting neutrons at  $E_n = 262$  keV<sup>17</sup>.

## 2. Experimental method

The experimental system is shown schematically in Fig. 1 where the  $\gamma$  source is produced by either the  $V(n,\gamma)$  reaction or the  $\text{Fe}(n,\gamma)$  reaction. The lifetime of the compound nucleus produced by thermal neutron capture is of the order of  $10^{-14}$  sec, i.e., it decays promptly emitting  $\gamma$ - rays (in the case of bound levels) or both  $\gamma$ -rays and neutrons (for unbound levels).

Such  $\gamma$  sources are of huge intensities<sup>11</sup> being produced using kilogram amounts of the metal mounted in tangential beam tubes, near but outside the core of the Israel Research Reactor (IRR-2), where the typical thermal neutron flux is of the order  $\sim 2.6 \times 10^{12}$  n/cm<sup>2</sup>/s.

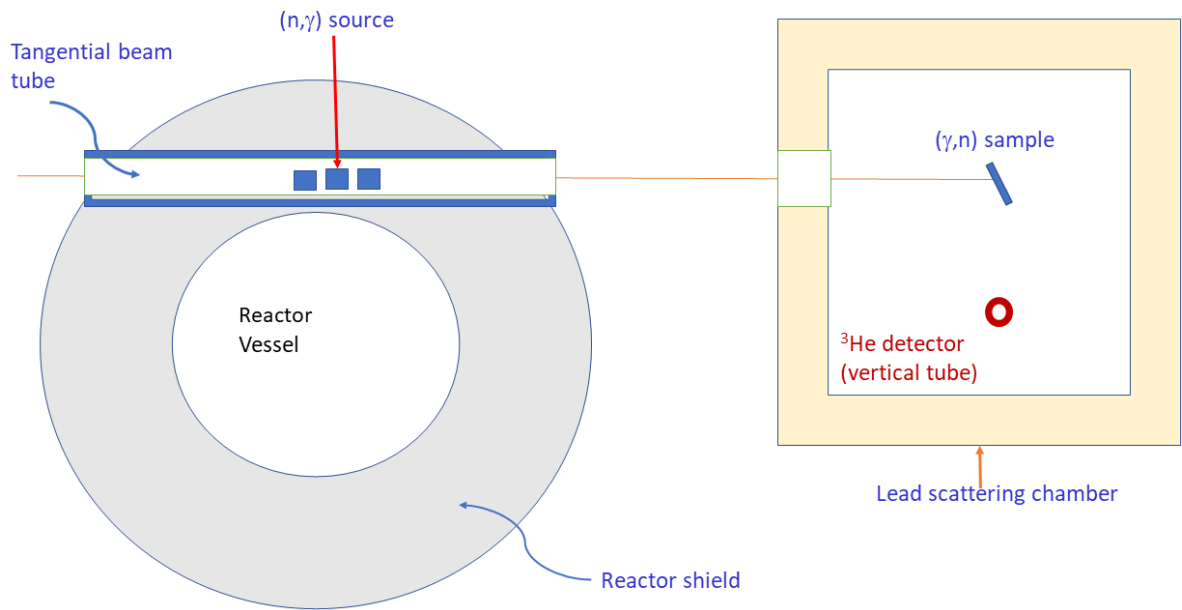


**Fig. 1. Schematic diagram of the experimental setup (not to scale) showing the (n,γ) source set inside a beam tube tangential to the reactor core. The high intensity γ-beam was neutron filtered using a 40 cm borated paraffin absorber (for reducing the neutron background inside the scattering chamber). The scattering chamber is surrounded by walls of a 15 cm thick lead shielding.**

The V(n,γ) source was in the form of 6 separated metallic discs each 1 cm thick and 8 cm diameter with a spacing of 2 cm from each other. The discs were placed near the Reactor core and along a beam tube *tangential* to the reactor core. The resulting γ beam was collimated and neutron filtered yielding intensities of  $\sim 10^6$  photons/cm<sup>2</sup>/sec (for the strong γ lines) at the target position. The distance between the (n,γ) source and the target position is  $\sim 6$  m. The <sup>3</sup>He detector, placed at 27 cm from the target, is a commercial neutron detector manufactured by Seforad-Applied Radiation Ltd., Emek Hayarden, Israel<sup>18,4</sup>. This detector consists of a cylindrical, gridded ionization counter of Shalev-Cuttler<sup>18</sup> type (5 cm diameter and 15 cm active height) filled with 6 atm of <sup>3</sup>He and 3 atm of argon and 0.5 atm of methane. Neutron detection relies on the <sup>3</sup>He(n,p)T reaction where  $Q = 764$  keV. For *thermal neutrons* the absorption cross section is huge, 5300 b, producing a strong peak at 764 keV in the neutron spectrum. This peak (not shown in Fig. 4 and Fig. 7) corresponds to the energy sum of the emitted p and T ions deposited in the ionization chamber. The energy scale of the fast neutrons is selected in such a way that its *zero value* starts at the peak of thermal neutrons. Details of energy calibration are described in Ref.14.

The signals from the <sup>3</sup>He n-detector, were fed through a pre-amplifier to a shaping main amplifier producing gaussian shaped signals. The pulses from the amplifier were sorted using a Canberra

80 Analyzer where the obtained pulse height spectra could be analyzed for peak area calculation and energy calibration. The best energy resolution was obtained by operating the amplifier with a time constant  $\tau \sim 12.8 \mu\text{s}$ . It was beneficial to increase  $\tau$  with increasing neutron energy to allow for a better charge collection of the  $^3\text{He}$  detector. During the measurements the observed counting rate was lower than about 3000 cps, mainly due to the good collimation of the incoming gamma beam and to the target detector distance. Hence, no serious pileup effects were observed.

It should be emphasized that the use of a *tangential* beam tube is of paramount importance and one should avoid using a *radial* beam tube for producing the gamma source. This is because in a *radial* beam the amount of gamma and neutron background emerging from the reactor core is so huge that it overwhelms any gamma signal emitted by the  $(n, \gamma)$  reactions.

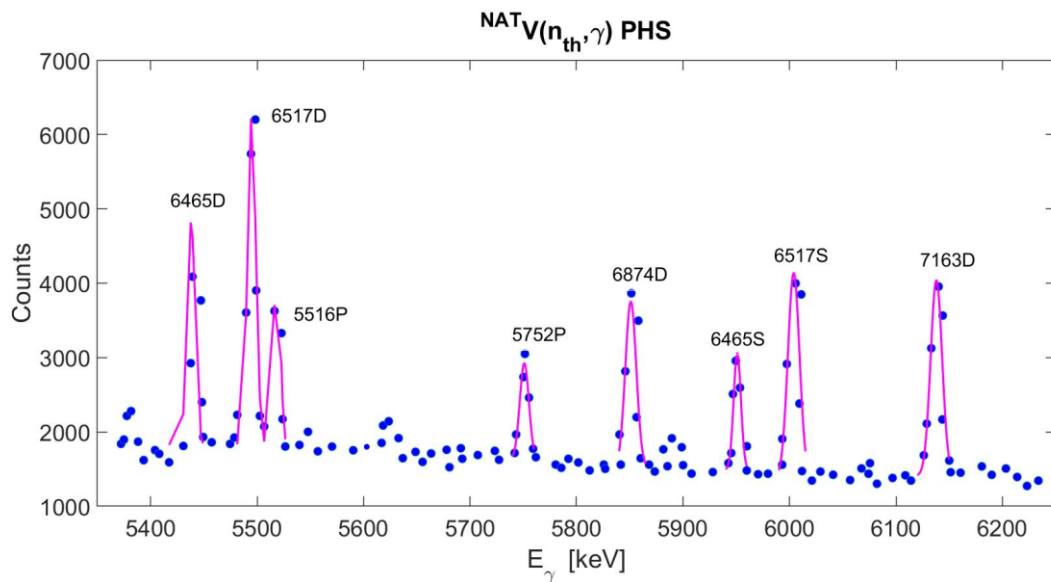


**Fig. 2.** High energy part of  $V(n_{th}, \gamma)$  pulse height spectrum (PHS), measured using a relatively small Ge detector (40cc), hence the double escape peaks (noted by D) have the strongest intensities (S = single escape, P = photopeak). The measurement was carried out by mounting the Ge detector at the position of the  $(\gamma, n)$  sample and inserting a 20 cm thick Pb attenuator for reducing the  $\gamma$ -line intensities to levels tolerated by the Ge detector. The strong intensity  $V$   $\gamma$ -lines are emphasized by Gaussians fitted to the measured points.

Fig. 2 shows the high energy part of the  $V(n, \gamma)$  spectrum in the energy range 4 to 7.5 MeV as measured using a 40 cc Ge detector in conjunction with a multichannel analyzer. The direct  $\gamma$ -beam was passed through a 40 cm borated paraffin absorber (not shown in Fig. 1); located along the tangential beam tube, for reducing the neutron background inside the scattering chamber. The

strong intensity  $\gamma$  line at 7163 keV is responsible for the photoexcitation of a resonance level in  $^{207}\text{Pb}$  followed by emitting neutrons with an energy of 423 keV.

### 3. Results

#### 3.1. The 423 keV neutron source

As mentioned above, only the 7163  $\gamma$ -line of the  $V(n,\gamma)$  reaction photoexcites resonantly by chance a nuclear level in  $^{207}\text{Pb}$ . This level is unbound with a neutron separation energy of 6738 keV, decaying by neutrons with an energy of  $E_n = 423$  keV, and proceeding to the ground state of  $^{206}\text{Pb}$ . The neutron generation process is described in Fig. 3 and the corresponding pulse height spectrum (PHS) as measured using the high resolution  $^3\text{He}$  detector<sup>18</sup> is shown in Fig. 4; it has a resolution of 17 keV for thermal neutrons and 24 keV for 1 MeV neutrons. The neutron group appearing on channel 620 is due to a contamination of the V source with metallic Chromium known to exist in the tangential beam tube. This n-group could be avoided by removing the Chromium from the beam tube. At this time, we could not make any changes because the Cr source is highly radioactive after many years of irradiation inside the tangential beam tube. The detector was shielded by wrapping it with 0.5 mm of metallic Cd and 6 mm of metallic Pb.

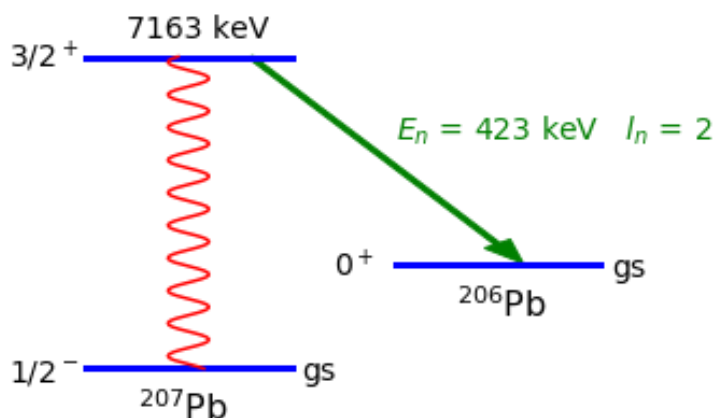
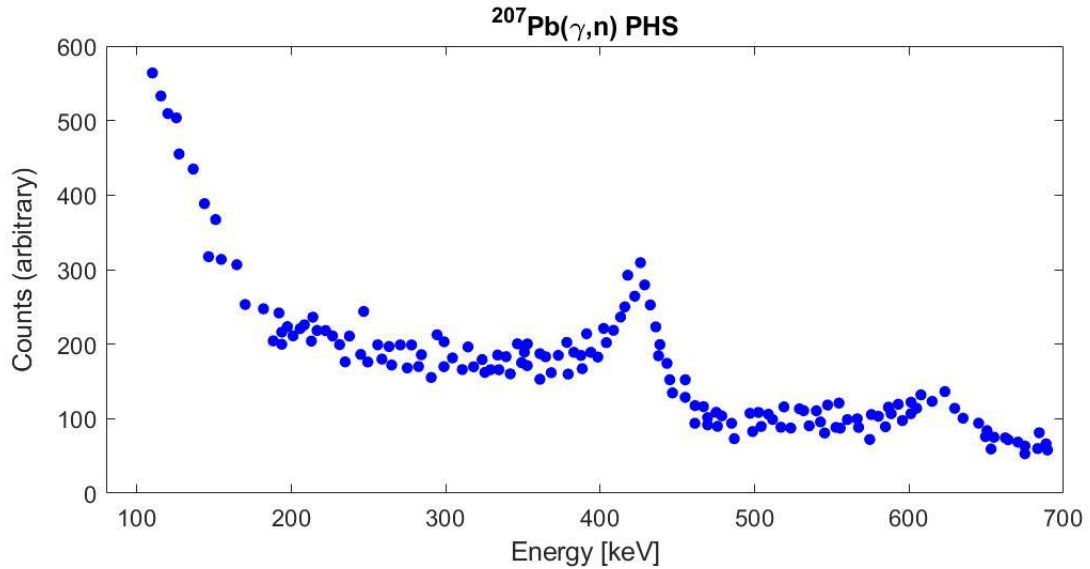


Fig. 3. Photoexcitation of the 7163 keV resonance level in  $^{207}\text{Pb}$  showing the photo absorption process and the subsequent 423 keV neutron emission (with  $l_n = 2$ ) leading to the  $^{206}\text{Pb}$  ground state,  $J_f^\pi = 0^+$ , via the  $^{207}\text{Pb}(\gamma,n)$  reaction.

In this measurement the  $^{207}\text{Pb}$  enriched target ( $^{207}\text{Pb}$  92.4%, 5.5%  $^{208}\text{Pb}$ ,  $^{206}\text{Pb}$  2.1%) was a 11.17 g square shaped (3.5 cm) in the form of powdered  $\text{PbCO}_3$  containing a net weight of 8.0 g of  $^{207}\text{Pb}$ ; it was inclined at 45 deg relative to the incident  $\gamma$ -beam and enclosed inside a very thin plastic film.



**Fig. 4.** Pulse height photoneutron spectrum of the  $^{207}\text{Pb}(\gamma,n)$  reaction as measured using the  $^3\text{He}$  detector. The neutron peak is at an energy of 423 keV. The n-group at channel 620 is due to a contamination of the V source with metallic Chromium known to be present in the tangential beam port. Channel zero corresponds to the energy of the thermal neutron peak (see text).

In order to determine the angular momentum of the emitted neutrons, it was necessary to measure the angular distribution; the results taken at 5 angles between  $50^\circ$  and  $130^\circ$  (using a running time of around 1 week per angle) was found to be symmetric around  $90^\circ$  (see Fig. 5) which is characteristic of n-emission from a resonance level<sup>16,17,20</sup>. It was fitted to an expansion of even Legendre polynomials using only the first two terms:

$$W(\theta) = A_0 + A_2P_2(\cos\theta) \quad (1)$$

Where  $\theta$  is the angle between the incident photon beam and the emitted neutron in the scattering plane; the deduced ratio was:  $A_2/A_0 = -0.538 \pm 0.055$ . To check whether there is a departure from symmetry we carried out a goodness of fit test using the data of Fig. 5; the statistics is:  $\chi^2 = 7.51$ . The critical value for the  $\chi^2$  distribution with 4 degrees of freedom at the customary 5% significance level is 9.49. Therefore, a symmetric Legendre polynomial describes satisfactorily the measured data, with a p-value of about 11.1%, higher than the significance level of 5% (even

higher than a more stringent significance level of 10%). In addition, any asymmetry in the angular distribution may be caused by a mixture of two different multiplicities in the formation of the level which is unlikely to occur in the present case.

This angular distribution corresponds to an emitted neutron with an angular momentum  $l_n = 2$ . Since the ground state of  $^{207}\text{Pb}$  is  $J_0^\pi = 1/2^-$ ; hence denoting by  $J$  the spin of the emitting resonance level in  $^{207}\text{Pb}$ , the conservation of angular momenta requires that:  $J + l_n + s_n = J_f$ , where  $s_n$  is the neutron spin and  $J_f$  is the ground state spin of the final nucleus.

Hence, to conserve parity and angular momentum, it seems that the resonance level at 7163 keV in  $^{207}\text{Pb}$  has a spin and parity of  $J^\pi = 3/2^+$  (being photoexcited by  $E1$  transition) and the emitted neutron proceeds with  $l_n = 2$  to the  $^{206}\text{Pb}$  ground state having  $J_f^\pi = 0^+$ .

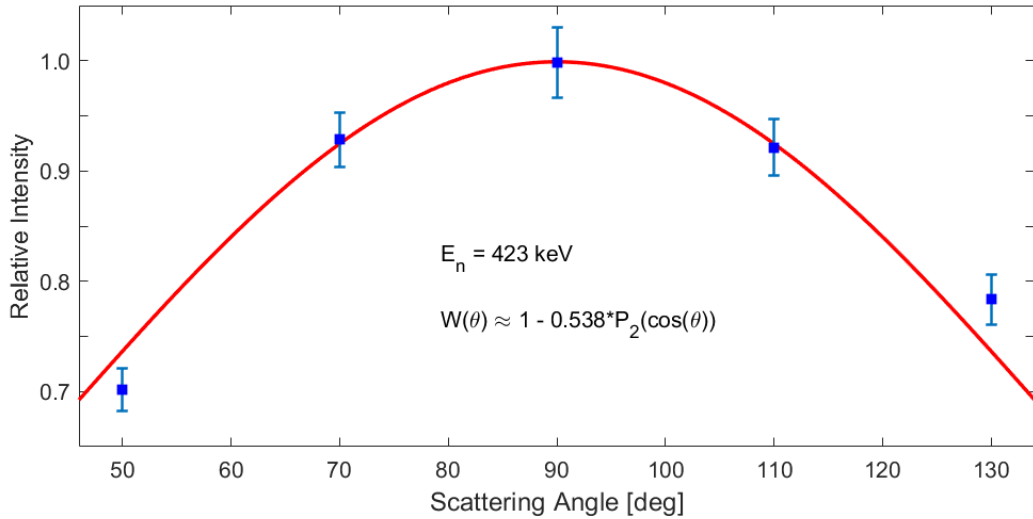


**Fig. 5. Angular distribution of the resonance neutron group at 423 keV measured using the  $^3\text{He}$  neutron detector. The error in the  $A_2$  parameter is about 10%.**

The resonance process has a relatively high scattering cross section for emitting neutrons and hence may be utilized as a new dynamic neutron source. The  $(\gamma, n)$  differential cross section was measured relative to that of the 86 keV source by accounting for the relative efficiencies using the following relation:

$$\left(\frac{d\sigma}{d\Omega}\right)_{En} = \frac{Y_\theta^{En}}{Y_\theta^{86}} \frac{\mathcal{N}_{86}}{\mathcal{N}_{En}} \frac{\epsilon_n^{En}}{\epsilon_n^{86}} \left(\frac{d\sigma}{d\Omega}\right)_{86} \quad (2)$$

Where  $Y$  are the measured yields normalized per unit time, at 86 keV<sup>14</sup> and at a neutron energy  $E_n$  respectively,  $\mathcal{N}$  is the number of nuclei in the two targets (respectively), while  $\epsilon$  are the

relative efficiencies taken from Franz<sup>19</sup> as mentioned above. This relation is applicable for cases where the setups of the two measurements are exactly the same. The number of nuclei ratio is relevant only for the <sup>205</sup>Tl target case and was found to be 1.078. To obtain the total cross section it is necessary to account for the angular distribution of the neutrons. The errors in the efficiencies taken from Franz<sup>19</sup> at 120 keV and 460 keV, are 6% and 5.5% respectively. Thus, the  $\sigma(\gamma,n)$  cross section for the 7163 keV resonance in <sup>207</sup>Pb was found to be  $\sigma(\gamma,n) = 35 \pm 6$  mb. The intensity of the 423 keV neutron source was equal to  $2.0 \times 10^3$  n/sec.

Due to the recoil of the final nucleus (<sup>206</sup>Pb), the energy of the emitted neutrons from the <sup>207</sup>Pb( $\gamma,n$ ) reaction varies with the n-emission angle relative to the incident  $\gamma$ -beam. The energy spread of the 423 keV neutrons reaching the <sup>3</sup>He n-detector at 90° was calculated to be:  $\pm 80$  eV corresponding to an angular spread of  $\pm 6^\circ$  subtended by the detector.

### 3.2. The 99 keV neutron source

The iron  $\gamma$ -source was in the form of 5 metallic discs each 2 cm thick and 8 cm diameter with a spacing of 2 cm from each other. The Fe discs were placed in a separate tangential beam tube and near the core of the IRR-2 reactor. The generation process of this neutron source based on the Fe(n, $\gamma$ ) is described in Fig. 6 where the emitting isotope is <sup>205</sup>Tl. A 10.4 g disk shaped metallic Tl sample of 4.0 cm diameter was used inclined at 45 deg relative to the incident gamma beam. Natural Tl consists of two isotopes <sup>205</sup>Tl (70.5%) and <sup>203</sup>Tl (29.5%). Only <sup>205</sup>Tl was shown to resonantly scatter the 7646 keV  $\gamma$  line of the Fe(n, $\gamma$ ) reaction (Ref. 11). This level in <sup>205</sup>Tl is unbound and is known to decay by two channels: photons and neutrons. The photon decay proceeds elastically to the ground state in <sup>205</sup>Tl and inelastically to excited states as reported in detail in Ref. 11. This level also emits 99 keV neutrons leading to the ground state of <sup>204</sup>Tl. The neutron spectrum as measured using the <sup>3</sup>He detector is shown in Fig. 7.

The angular distribution of the resonantly scattered 7646 keV *photons* was measured<sup>11</sup> and found to be isotropic. Since the ground state spin in <sup>205</sup>Tl is  $1/2^+$  hence the 7646 keV level is very likely  $J^\pi = 1/2^-$  because of its large width which is characteristic of *E1* transitions. It follows that the emitted neutrons proceed to the  $J_f^\pi = 2^-$  ground state of <sup>204</sup>Tl by a d-wave transition,  $l_n = 2$  (see Fig. 6), thus conserving both parity and angular momentum as in the case of the 423 keV neutron group. The  $\sigma(\gamma,n)$  cross section for the 7646 keV resonance in <sup>205</sup>Tl was determined relative to that of the 86 keV neutron source<sup>14</sup> and found to be  $\sigma(\gamma,n) = 107 \pm 17$  mb where the error arises

from the statistics of both the neutron signal and the background. Thus the intensity of this neutron source was found to be  $\sim 4.0 \times 10^4$  n/sec.

The total energy spread of this neutron group, between the forward to backward emitted neutrons, is 1.1 keV. Here, the measurement of the 99 keV neutrons is at  $90^\circ$  with an angular opening of  $^3\text{He}$  detector of  $\pm 6^\circ$  which corresponds to a neutron energy spread of  $\pm 39$  eV.

### 3.3. Doppler broadening

Both the incident 7163  $\gamma$ -line of the  $V(n,\gamma)$  reaction and the nuclear level in  $^{207}\text{Pb}$  are Doppler broadened. The broadening is given by:  $\Delta = E_\gamma(2kT_e/Mc^2)^{1/2}$ , where  $E_\gamma = 7163$  keV, the energy of the incident line of the  $\gamma$ -source,  $k$  is the Boltzmann constant and  $M=51$  is the Vanadium atomic mass.  $T_e$  is the effective temperature of metallic V, where the ambient temperature

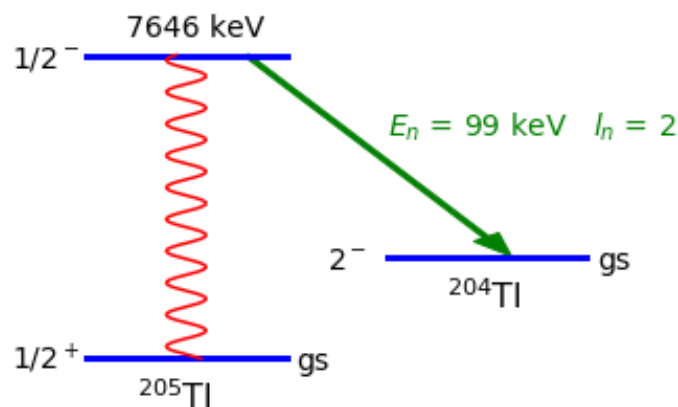
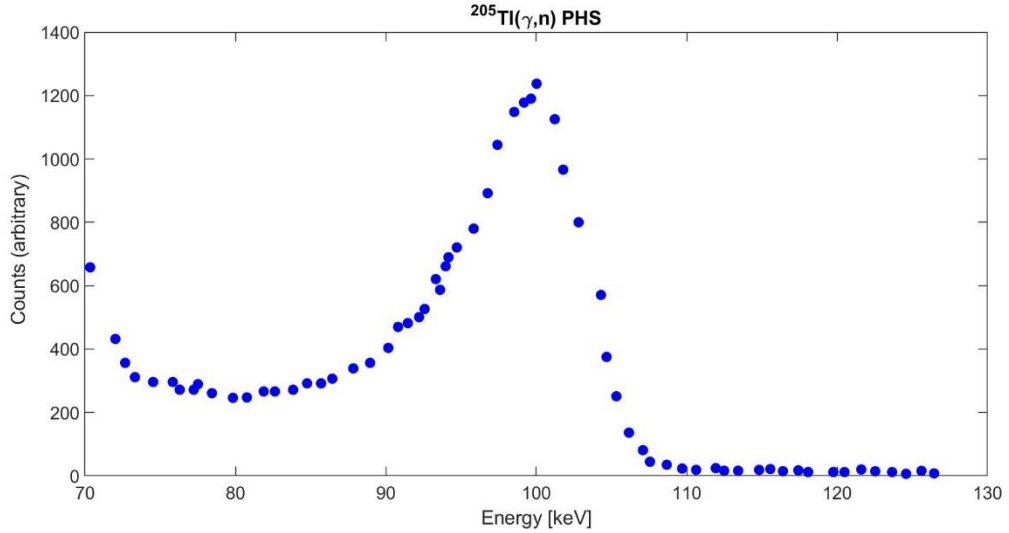


Fig. 6. Photoexcitation of the 7646 keV resonance level in  $^{205}\text{Tl}$  showing the photo absorption process and the subsequent 99 keV neutron emission (with  $l_n=2$ ) leading to the  $^{204}\text{Tl}$  ground state,  $J_f^\pi = 2^-$ , via the  $^{205}\text{Tl}(\gamma,n)$  reaction.



**Fig. 7. Pulse height photoneutron spectrum emitted by the 7646 keV photoexcited level in  $^{205}\text{Tl}$  as measured using the  $^3\text{He}$  detector. The neutron peak is at an energy of 99 keV.**

during reactor operation, is  $T = 550$  K. To calculate  $T_e$  for metallic V, we used the Lamb formula<sup>22</sup>, which requires a knowledge of the Debye temperature of Vanadium,  $\Theta_D(\text{V}) = 390$  K, from which we get  $T_e = 560$  K at  $T = 550$  K, yielding a spread of  $\Delta_s = 10.2$  eV, for the  $\gamma$ -line source. Similarly, the Doppler width of the resonance level in  $^{207}\text{Pb}$  is  $\Delta_r = 3.8$  eV; being smaller because  $M = 207$  and  $T_e = 300$  K (obtained using a Debye temperature,  $\Theta_D(\text{Pb}) = 87$  K) assuming a sample temperature of  $T = 298$  K. Here however, this level is unbound having  $\Gamma_n > 0$  with a total width  $\Gamma = \Gamma_n + \Delta_r$ .

The kinematics of the  $(\gamma, n)$  reaction causes a broadening of the emitted neutrons which depends on the angle of n-emission with respect to the incident  $\gamma$ -beam direction. As shown above, the energy spread of the 99 keV group is  $\pm 39$  eV which is larger than the thermal Doppler broadening.

In the same manner, the results of the Fe-Tl combination were calculated yielding:  $\Delta_s = 11.5$  eV (for the 7646  $\gamma$ -line source) and  $\Delta_r = 4.1$  eV the Doppler width of the  $^{205}\text{Tl}$  nuclear level. Here also the total level width includes the neutron width of the 7646 keV level.

Such dynamic neutron sources can be used for energy and efficiency calibrations of n-detectors and also for n-scattering experiments.

#### 4. Background

#### 4.1 Background subtraction

A linear smooth non-resonant n-background was subtracted from below the resonance peaks. This procedure is justified by noting that all non-resonant samples of neighboring Z produced a similar smooth *non-peaked* background. The procedure is illustrated in Fig. 8 for the 423 keV case. A Gaussian plus a smooth linear background was fitted to the peak. Using the obtained parameters integration was performed in the energy range 380-460 keV yielding a background of 11195 and a net area of 4912, hence a statistical error of 2.6%. The peak at 99 keV is stronger with a relative smaller background yielding a statistical error of 1.2% (integration in the energy range 85-110 keV).

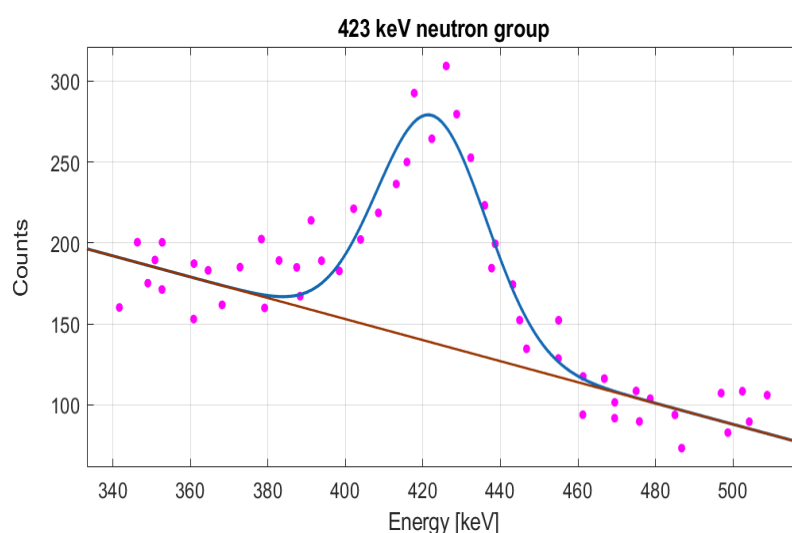


**Fig. 8. Background subtraction and analysis of the neutron group at 423 keV.**

In calculating the total error in the  $(\gamma, n)$  cross sections we also accounted for the 6% errors in the relative efficiencies of the  $^3\text{He}$  detector, the error in the reference cross section at 86 keV resonance (13.5%) and the error in the integrated angular distribution (2.3% - obtained by drawing 1000 samples of its parameters from normal distributions and averaging). All of which added quadratically. The statistical counting errors play a small role compared with the reference cross section error and the relative efficiency errors and, therefore, both measured cross sections came out with a 16% error. Hence, the measured  $(\gamma, n)$  cross sections were found to be  $35 \pm 6$  mb (accounting also for the 1.078 ratio of the nuclei in the targets) for the 423 keV resonance and  $107 \pm 17$  mb for the 99 keV resonance.

## 4.2 Neutron background

We hereby deal with the neutron and gamma background in the scattering chamber. The n-background reaching the scattering chamber from the walls of the tangential beam tube during reactor operation is very small because of the 40 cm long borated paraffin which seem to be a very effective neutron shield. The neutrons within the scattering chamber are created mainly via the  $(\gamma,n)$  reaction on the sample and partly by the  $(\gamma,n)$  reaction on the lead collimators and shielding. The direct beam of the vanadium capture  $\gamma$ -rays consists of strong intensity lines at 6874, 7163, 7311 keV which are higher than the  $(\gamma,n)$  threshold of  $^{207}\text{Pb}$ . Neutrons are emitted not only resonantly as in the case of the 7163 keV line but also, to a lesser extent and with a much smaller cross section, via a photoneutron process from the tail of the giant dipole resonance. Such emitted neutrons increase the  $\gamma$ -background via the  $(n,\gamma)$  reaction on the structural materials of the detector and of the lead shielding surrounding the detector.

In the present work, we routinely measured the neutron background in the absence of the resonant target. This was usually found to be small, of  $\sim 7\%$  of the original neutron peak. In the following we use a Monte Carlo calculation to deal with the effect of neutron multiple scattering (MS) on the Pb shielding walls of the scattering chamber.

## 4.3 Neutron multiple scattering

The neutron MS from the lead walls, was evaluated by a Monte Carlo simulation (using the MCNP code) for a 0.4 MeV neutron beam shooting forward (in a  $60^\circ$  angle to shield the detector from the original neutrons) at a 15 cm thick lead wall at a distance of 60 cm (which is closely our experimental conditions); the result given in Fig. 9 below shows that there are indeed only about  $1.47 \times 10^{-5} \%$  background neutrons at the nominal energy of the beam and a total of  $2.5 \times 10^{-5} \%$  for all the produced energies. We estimated, by a separate simulation, that a flux of  $10^5$  neutrons will enter the scattering chamber from the reactor. Combined with a hole of radius 10 cm in the scattering chamber wall close to the reactor (meaning a fluence of  $3.1 \times 10^7$ ), and with the above probability of detecting the backscattered neutrons, we found that the background is  $\sim 8$  neutrons/sec. The majority of these neutrons, coming from the tangential beam tube outside the core, are at thermal or low epithermal energy, well below the energies of interest in the present

work. This shows that the background effect caused by MS of neutrons is insignificant and can be neglected.

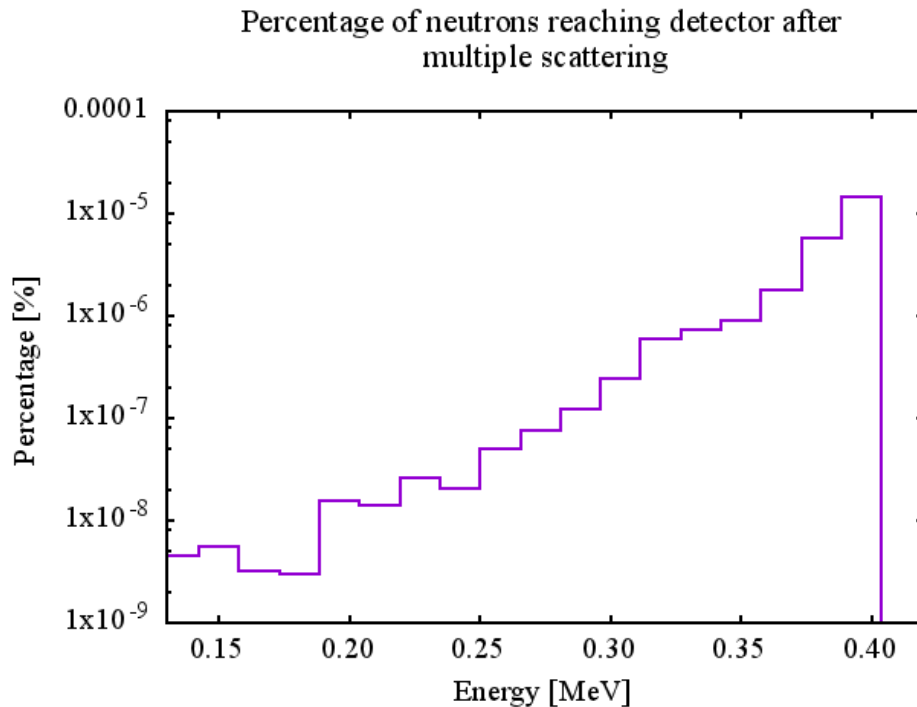


**Fig. 9. Percentage of neutrons reaching the <sup>3</sup>He detector after multiple scattering. The incident n-energy is assumed to be 0.4 MeV.**

#### 4.4 Effect of Photon Contamination

The two neutron sources are contaminated with low energy photons of ~ 0.5 MeV produced by Compton scattering at 90° of the high intensity lines of the  $\gamma$ -sources on the high Z targets and by the 0.511 MeV photons obtained by positron annihilation. The electron-positron pairs are produced by the dominant pair-production process of the high energy photons ( $E_\gamma > 5$  MeV) with the ( $\gamma, n$ ) targets. More than 90% of those photons are absorbed by the 6 mm Pb shield around the <sup>3</sup>He detector. So, the effect of the low energy photons was quite insignificant.

It is also important to remember that individual electrons cannot deposit more than ~ 300 keV in the <sup>3</sup>He gas, and such pulses have amplitudes well below the thermal peak.

We now discuss the effect of photon contamination of the 99 keV neutron source. In addition to the low energy photons, this n-source is also contaminated with high energy photons contributed by the <sup>205</sup>Tl isotope being a strong resonance scatterer of the 7646 keV  $\gamma$ -line of the Fe(n, $\gamma$ ) reaction<sup>11</sup> with a  $\gamma$ -scattering cross section of 0.59 b. The effect of such photon contamination on

the detection of the 99 keV neutrons is much smaller in comparison to that of the 86 keV n-source<sup>14</sup> which is by far strongly contaminated by the 7279 keV  $\gamma$ -line (emitted by the Fe(n, $\gamma$ ) source) and known<sup>21</sup> to be resonantly scattered by <sup>208</sup>Pb having a huge scattering cross section of 5.6 b. Since the resolution of the 86 keV neutron line, as measured by the <sup>3</sup>He detector, was not affected<sup>14</sup> by such a strong intensity high energy photon contaminant, one would expect a negligible effect on the 99 keV neutron peak also.

The n- and  $\gamma$ -backgrounds of the 99 keV n-source are in principle higher than the 423 keV n-source. This is because the Fe(n, $\gamma$ ) source has strong intensity  $\gamma$ -lines at higher energies: 7279, 7632, 7646 and 9298 keV, producing higher neutron yields, being above the ( $\gamma$ ,n) threshold for some stable isotopes of Tl. This causes an increase in the n- and hence of the  $\gamma$ -background via the (n, $\gamma$ ) reaction. However, this higher background was small relative to the strong intensity of 99 keV neutron peak created by the <sup>205</sup>Tl( $\gamma$ ,n) reaction.

The transmission through 0.5 mm Cd is 98.2% and 98.3% for respectively 99 and 423 keV neutrons. For 6 mm lead it is 79.9%, 82.4% and 88.8% at thermal, 99 and 423 keV energies. These numbers were obtained using a Monte Carlo simulation.

## 5. Increasing the intensity of the neutron sources

The intensity of the 99 keV n-source (produced by the Fe-<sup>205</sup>Tl combination) can, in principle, be increased by a factor of  $\sim 300$  i.e. to  $\sim 2 \times 10^7$  n/sec by using a larger mass (100 g) of the ( $\gamma$ ,n) target of Tl with a larger diameter  $\sim 6.0$  cm and employing a higher n-flux reactor of  $\sim 10^{14}$  n/cm<sup>2</sup>/s and if possible, a shorter distance of  $\sim 5$  m between the  $\gamma$ -source and the ( $\gamma$ ,n) target. The use of a larger diameter of the Tl target is to diminish the attenuation of  $\gamma$ -ray intensity within the target. In a similar manner, the intensity of the 423 keV n-source created by the V-<sup>207</sup>Pb combination can be increased to  $\sim 6 \times 10^5$  n/sec by using a larger isotopic <sup>207</sup>Pb mass (of  $\sim 80$  g) in conjunction with a higher n-flux reactor of  $10^{14}$  n/cm<sup>2</sup>/s. But it should be stressed that there is a very strong dependence on the type of the reactor available and its geometry. Not two reactors are the same and it should not be expected to receive exactly the numbers of the present paper at other installations.

## 6. Conclusions

It is shown that two relatively strong and quasi monoenergetic neutron sources with energies of 99 keV and 423 keV can be produced, at a nuclear reactor, using a combination of (n, $\gamma$ ) and ( $\gamma$ ,n) reactions. The method depends on a chance overlap between a discrete  $\gamma$ -line produced by n-capture on V or Fe and *isolated* resonance levels in  $^{207}\text{Pb}$  and  $^{205}\text{Tl}$  respectively.

The energy spread of the such neutron sources is of particular interest because each source is nearly monochromatic, the first at  $\sim 100$  keV and the second at  $\sim 400$  keV. These are quite different from the conventional n-sources<sup>23</sup> such as that of  $^{252}\text{Cf}$  which is spread over a wide energy range of 10 eV to 10 MeV or the  $^{241}\text{AmBe}$  source covering the 100 eV to 10 MeV region.

## References

1. K. H. Beckurts, K. Wirtz, Neutron Physics (translated from the second German edition (1964) by L. Dresner), Springer-Verlag, New York, 1964.
2. A. N. Garg, R. J. Batra, J. Radioanalytical Nucl. Chem., **98** (1986) 167.
3. M. Fujishiro, T. Tabata, K. Okamoto, T. Tsujimoto, Can. J. Phys., **60** (1982) 1672.
4. Glenn Knoll, Radiation Detection and Measurement, John Wiley & Sons, 2010.
5. D. A. Allen, T. D. Beynon, Med. Phys. **27** (2000) 1113.
6. C. Andreani, D. Colognesi, J. Mayers, G. F. Reiter, R. Senesi, Adv. Phys. **54** (2005) 377.
7. C. Guerrero et al., Eur. Phys. J., **A49** (2013) 27.
8. K. A. Alfieri, R.C. Block, R.J. Turinsky, Nucl. Sci. Eng. **51** (1973) 25.
9. R. Moreh, R.C. Block, Y. Danon, Nuc. Inst. Meth. in Phys Research **A 562** (2006) 401.
10. M. A. Lone, R.A. Leavitt, D.A. Harrison, Atomic Data and Nucl. Data Tables, **26** (1981) 511.
11. R. Moreh, A. Wolf, Phys. Rev. **182** (1969) 1236.
12. M. Wang, G. Audi, F.G. Kondev, W.J. Huang, S. Naimi, X. Xu, Chinese Physics C, **41** (2017) 030003.
13. J.E. McFee, W.V. Prestwich, T.J. Kennett, Phys. Rev. **C13** (1976) 1864.
14. R. Moreh, Y. Birenbaum, Z. Berant, Nucl. Inst. Meth., **155** (1978) 429.

15. R. Moreh, R. Fedorowicz, W.V. Prestwich, T.J. Kennett, M.A. Islam: Nucl. Inst. Meth. **A309** (1991) 503.
16. Z. Berant, Y. Birenbaum, R. Moreh, O. Shahal, Nucl. Phys., **A368** (1981) 201.
17. Y. Birenbaum, Z. Berant, S. Kahane, R. Moreh, A. Wolf, Nucl. Phys. **A369** (1981) 483.
18. S. Shalev, J. Cuttler, Nucl. Sci. Eng. **51** (1973) 52.
19. H. Franz et al., Nucl. Inst. Meth. **144** (1977) 253.
20. D. J. Horen, J.A. Harvey, N.W. Hill, Phys. Rev. **C18** (1978) 722.
21. R. Moreh, S. Shlomo, A. Wolf, Phys. Rev. **C2** (1970) 1144.
22. W. E. Lamb, Jr., Phys. Rev. **55** (1939) 190.
23. E. A. Lorch, Intern. J. Appl., Rad. Isot. **24** (1973) 585-591.